

# The capacitance of the circular parallel plate capacitor obtained by solving the Love integral equation using an analytic expansion of the kernel

Martin Norgren and B. L. G. Jonsson

September 21, 2009

Division of Electromagnetic Engineering  
Royal Institute of Technology  
SE-100 44 Stockholm, Sweden

Corresponding author: Martin Norgren  
Email: martin.norgren@ee.kth.se  
Tel: +46 8 7907410; Fax: +46 8 205268

## Abstract

The capacitance of the circular parallel plate capacitor is calculated by expanding the solution to the Love integral equation into a Fourier cosine series. Previously, this kind of expansion has been carried out numerically, resulting in accuracy problems at small plate separations. We show that this bottleneck can be alleviated, by calculating all expansion integrals analytically in terms of the Sine and Cosine integrals. Hence, we can, in the approximation of the kernel, use considerably larger matrices, resulting in improved numerical accuracy for the capacitance. In order to improve the accuracy at the smallest separations, we develop a heuristic extrapolation scheme that takes into account the convergence properties of the algorithm. Our results are compared with other numerical results from the literature and with the Kirchhoff result. Error estimates are presented, from which we conclude that our results is a substantial improvement compared with earlier numerical results.

## 1 Introduction

The exact capacitance of the circular parallel plate capacitor, with infinitely thin plates, remains an unsolved problem in potential theory, in the sense that to this date no explicit analytical solution has been reported. However, the problem can be formulated as a Fredholm integral equation of the second kind, known as Love's integral equation [1], which can be solved numerically.

To our knowledge, the up to date most accurate studies of the capacitance at small plate separations are the ones by Wintle and Kurylowicz [2] and by Carlson and Illman [3]. Both of these studies have been used as benchmarks for solutions obtained by other methods; see e.g. [4–6]. Wintle and Kurylowicz [2] use an El-Gendi method [7] to rewrite the Love equation and apply numerical integration using the Clenshaw-Curtis quadrature method [8] to obtain the capacitance. Carlson and Illman [3] solve the Love equation through an expansion of the kernel into a Fourier-cosine series. Later, they have also extended that method to solve the three-plate problem by means of coupled Love type equations [9]. It is known [1] that for small plate separations, a solution obtained via a series expansion of the kernel converges slowly, requiring a large number of expansion terms. To calculate the expansion coefficients of the kernel, Carlson and Illman [3] use numerical integration. Hence, their method is limited by a combination of the accuracy of the integration and the large number of terms needed. The accumulated errors effectively limit the expansion to about 100 terms, which is insufficient for convergence at very small separations.

In this paper, we show that all of the integrals in the series expansion in [3] can be expressed analytically in terms of the well-studied Sine- and Cosine integrals. In this way, we improve the numerical accuracy of the expansion coefficients up to the accuracy of the evaluations of the Sine- and Cosine integrals, which makes it possible to increase the number of expansion functions considerably. Hence, in our method, the numerical accuracy in the capacitance is mainly limited by the truncation of the number of expansion functions. Thus, we can present improved results for the capacitance at small plate separations; results that surpass the results in [2, 3], both in correctness and in the significant numbers of digits. Our results are also in excellent agreement with the result by Kirchhoff [10],

which becomes increasingly accurate when the plate separation tends to zero [11, 12].

The paper is organized as follows: In Section 2, we review the expansion method, originally presented in [3]. In Section 3, we derive the analytical expressions for all the expansion integrals. Numerical results are presented in Section 4 and Section 5 contains some conclusions.

## 2 Problem formulation and initial analysis

The circular parallel plate capacitor is depicted in Figure 1. The distance between the circular plates is denoted  $d$  and their common radius is denoted  $a$ . The model is idealized in the sense that the plates have zero thicknesses. Following the notation used in many of the previous studies of this problem, we let  $\kappa = d/a$  denote the normalized separation between the plates.

The capacitance of the parallel plate capacitor is [3]

$$C = 4\epsilon_0 a \int_0^1 f(s) ds, \quad (1)$$

where the function  $f(s)$  is the solution to the modified Love integral equation

$$f(s) - \int_0^1 K(s, t) f(t) dt = 1, \quad 0 \leq s \leq 1, \quad (2)$$

with kernel

$$K(s, t) = \frac{\kappa}{\pi} \left[ \frac{1}{\kappa^2 + (s-t)^2} + \frac{1}{\kappa^2 + (s+t)^2} \right]. \quad (3)$$

Note that in the original derivation by Love [1], the kernel and the function are defined in the range  $-1 \leq s, t \leq 1$ , and the kernel has only one term, but since  $f(s)$  can be shown to be even one can instead use the formulations (2) and (3) (an elegant and short derivation of Love's integral equation can be found in [12]).

To solve Equation (2) numerically, we follow the approach in [3] and expand the kernel and the unknown function into the Fourier-cosine expansion functions

$$\psi_m(s) = \sqrt{2 - \delta_{m0}} \cos(m\pi s), \quad m = 0, 1, \dots, \quad (4)$$

which in our study have been normalized to fulfil the orthogonality relation

$$\int_0^1 \psi_m(s) \psi_{m'}(s) ds = \delta_{mm'}, \quad (5)$$

where  $\delta_{mm'}$  denotes the Kronecker delta function. Note that similarly to  $f(s)$  all  $\psi_m$ -functions have vanishing first derivatives at  $s = 0$ .

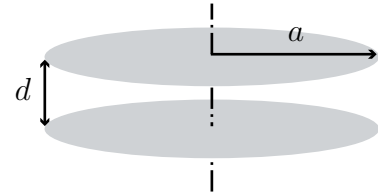


**Figure 1:** The circular parallel plate capacitor (side view slightly from above).

Carrying out the expansions of  $f(s)$  and  $K(s, t)$ , in terms of  $\{\psi_m\}$ , we obtain

$$f(s) = \sum_{m=0}^{\infty} f_m \psi_m(s), \quad (6)$$

$$f_m = \int_0^1 f(s) \psi_m(s) ds, \quad (7)$$

$$K(s, t) = \sum_{m=0}^{\infty} \sum_{n=0}^{\infty} K_{mn} \psi_m(s) \psi_n(t), \quad (8)$$

$$K_{mn} = \int_0^1 \int_0^1 K(s, t) \psi_m(s) \psi_n(t) ds dt, \quad (9)$$

which yield the following infinite linear system of equations for the coefficients  $\{f_n\}_{n=0}^{\infty}$ :

$$\sum_{n=0}^{\infty} (\delta_{mn} - K_{mn}) f_n = \delta_{m0}, \quad m = 0, 1, \dots \quad (10)$$

From (1), (6) and the orthogonality of (4), the capacitance reduces to

$$C = 4\epsilon_0 a f_0, \quad (11)$$

where  $f_0$  is simply the (0,0)-element in the inverse of the matrix with elements  $\delta_{mn} - K_{mn}$ . In the numerical implementation the matrix is truncated into the size  $0 \leq m, n \leq N$ , where we call  $N$  the truncation number. It is well-known [3, 11] that at small separations,  $\kappa$ , large values of  $N$  are required to obtain convergence of  $f_0$  in (11). Also, for the accuracy of the result, it is crucial that the matrix elements  $K_{mn}$ , given by the integrals in (9), have been calculated with a high accuracy.

For small values of  $\kappa$  the kernel  $K(s, t)$  has a pronounced crest at  $s = t$ , making it difficult to evaluate the integrals in (9) numerically. In [3] this problem has been alleviated, by adding and subtracting a suitable term to the kernel, thereby removing the crest in one of the integrals, and making the inner integral in the other integral available for explicit evaluation. A related procedure has also been used earlier in [2]. However, a remaining problem is that for large values of  $m, n$  the expansion functions (4) yield rapidly oscillating integrands, which (when integrated numerically) result in slow convergence and poor accuracy. Hence, it would be beneficial if all integrals, encountered when expanding the kernel, could be expressed analytically in terms of established functions, readily available for numerical evaluation with a high accuracy. In the next section we will show that this is indeed the case.

### 3 Expansion of the kernel into Sine and Cosine integrals

In this section, we derive the analytical expressions for the expansion of the kernel  $K(s, t)$ . First, we notice from (3) and (9) that the expansion coefficients have the property  $K_{nm} = K_{mn}$ , resulting in a symmetric matrix. For the special cases when the indices

coincide and/or becomes zero, it is advantageous for the numerical evaluation to derive special simplified expressions for  $K_{mn}$ . In most of the derivations, we utilize the following properties of the Sine and Cosine integrals [13]:

$$\text{Si}(z^*) = [\text{Si}(z)]^*, \quad (12)$$

$$\text{Ci}(z^*) = [\text{Ci}(z)]^*, \quad (13)$$

$$\text{Si}(-z) = -\text{Si}(z), \quad (14)$$

$$\text{Ci}(-z) = \text{Ci}(z) - j\pi \quad (0 < \arg z < \pi), \quad (15)$$

where  $*$  denotes complex conjugation and  $j$  denotes the imaginary unit.

### 3.1 Case $m = n = 0$

By elementary integrals, we obtain

$$\begin{aligned} K_{0,0} &= \int_0^1 \int_0^1 K(s, t) ds dt = \frac{\kappa}{\pi} \int_0^1 \left\{ \int_0^1 \left[ \frac{1}{\kappa^2 + (s-t)^2} + \frac{1}{\kappa^2 + (s+t)^2} \right] ds \right\} dt \\ &= \frac{1}{\pi} \int_0^1 \left[ \arctan\left(\frac{t+1}{\kappa}\right) - \arctan\left(\frac{t-1}{\kappa}\right) \right] dt \\ &= \frac{1}{2\pi} \left[ 4 \arctan\left(\frac{2}{\kappa}\right) - \kappa \ln\left(1 + \frac{4}{\kappa^2}\right) \right]. \end{aligned} \quad (16)$$

### 3.2 Cases $m = 0, n > 0$

Here the inner integral is the same as in the previous case, resulting in

$$\begin{aligned} K_{0n} &= \sqrt{2} \int_0^1 \int_0^1 K(s, t) \cos(n\pi t) ds dt \\ &= \frac{\sqrt{2}}{\pi} \int_0^1 \left[ \arctan\left(\frac{t+1}{\kappa}\right) - \arctan\left(\frac{t-1}{\kappa}\right) \right] \cos(n\pi t) dt. \end{aligned} \quad (17)$$

Defining the function

$$I_1(\beta, \kappa, \alpha) = \int_0^1 \cos(\beta t) \arctan\left(\frac{t+\alpha}{\kappa}\right) dt, \quad (18)$$

it follows that

$$K_{0n} = \frac{\sqrt{2}}{\pi} [I_1(n\pi, \kappa, 1) - I_1(n\pi, \kappa, -1)]. \quad (19)$$

By a change of variable and integration by parts, we obtain

$$\begin{aligned}
I_1(\beta, \kappa, \alpha) &= \int_0^1 \cos(\beta t) \arctan\left(\frac{t+\alpha}{\kappa}\right) dt = \left\{ u = \frac{t+\alpha}{\kappa} \right\} \\
&= \kappa \int_{\alpha/\kappa}^{(1+\alpha)/\kappa} \cos(\beta(\kappa u - \alpha)) \arctan(u) du \\
&= \frac{\sin(\beta)}{\beta} \arctan\left(\frac{1+\alpha}{\kappa}\right) - \frac{1}{\beta} \int_{\alpha/\kappa}^{(1+\alpha)/\kappa} \frac{\sin(\beta(\kappa u - \alpha))}{1+u^2} du \\
&= \frac{\sin(\beta)}{\beta} \arctan\left(\frac{1+\alpha}{\kappa}\right) \\
&\quad + \frac{1}{\beta} \text{Im} \left\{ \sin(\beta(\alpha + j\kappa)) (\text{Ci}(\beta(\alpha + j\kappa)) - \text{Ci}(\beta(\alpha + 1 + j\kappa))) \right. \\
&\quad \left. - \cos(\beta(\alpha + j\kappa)) (\text{Si}(\beta(\alpha + j\kappa)) - \text{Si}(\beta(\alpha + 1 + j\kappa))) \right\}. \quad (20)
\end{aligned}$$

The evaluation of the last integral was carried out in the Maple software, and the result was simplified using the trigonometric-hyperbolic addition formulas and the properties (12) and (13).

Insertion of (20) into (19) and further simplifications yield

$$K_{0n} = \frac{\sqrt{2}}{n\pi^2} \text{Im} \left\{ \cos(n\pi(1 + j\kappa)) \text{Si}(n\pi(2 + j\kappa)) + \cos(n\pi(1 - j\kappa)) \text{Si}(-jn\pi\kappa) \right. \\
\left. - \sin(n\pi(1 + j\kappa)) \text{Ci}(n\pi(2 + j\kappa)) - \sin(n\pi(1 - j\kappa)) \text{Ci}(-jn\pi\kappa) \right\}. \quad (21)$$

### 3.3 Cases $m \neq n, m > 0, n > 0$

Here, we obtain

$$\begin{aligned}
K_{mn} &= 2 \int_0^1 \int_0^1 K(s, t) \cos(n\pi t) \cos(m\pi s) dt ds \\
&= \frac{2}{\pi} \int_0^1 \int_0^1 \left[ \frac{\kappa}{\kappa^2 + (s-t)^2} + \frac{\kappa}{\kappa^2 + (s+t)^2} \right] \cos(n\pi t) \cos(m\pi s) dt ds. \quad (22)
\end{aligned}$$

Defining the function

$$I_2(\beta, \kappa, \alpha) = \int_0^1 \frac{\kappa \cos(\beta t)}{\kappa^2 + (t+\alpha)^2} dt, \quad (23)$$

it follows that

$$K_{mn} = \frac{2}{\pi} \int_0^1 [I_2(n\pi, \kappa, -s) + I_2(n\pi, \kappa, s)] \cos(m\pi s) ds. \quad (24)$$

Again, using Maple and some simplifications it follows that

$$\begin{aligned}
I_2(\beta, \kappa, \alpha) &= \text{Im} \left\{ \sin(\beta(\alpha + j\kappa)) (\text{Si}(\beta(\alpha + j\kappa)) - \text{Si}(\beta(\alpha + 1 + j\kappa))) \right. \\
&\quad \left. + \cos(\beta(\alpha + j\kappa)) (\text{Ci}(\beta(\alpha + j\kappa)) - \text{Ci}(\beta(\alpha + 1 + j\kappa))) \right\}. \quad (25)
\end{aligned}$$

Using (12)-(15), it follows that

$$\begin{aligned} I_2(\beta, \kappa, -s) + I_2(\beta, \kappa, s) &= -\text{Im} \left\{ \sin(\beta(s + j\kappa)) \text{Si}(\beta(s + 1 + j\kappa)) \right. \\ &\quad + \cos(\beta(s + j\kappa)) \text{Ci}(\beta(s + 1 + j\kappa)) \\ &\quad + \sin(\beta(s - j\kappa)) \text{Si}(\beta(s - 1 - j\kappa)) \\ &\quad \left. + \cos(\beta(s - j\kappa)) \text{Ci}(\beta(s - 1 - j\kappa)) \right\}. \end{aligned} \quad (26)$$

Inserting (26) into the expression (24) for  $K_{mn}$ , we can write

$$K_{mn} = \frac{2}{\pi} I_3(n\pi, \kappa, m\pi), \quad (27)$$

where the function

$$\begin{aligned} I_3(\beta, \kappa, \gamma) &= \int_0^1 [I_2(\beta, \kappa, -s) + I_2(\beta, \kappa, s)] \cos(\gamma s) ds = -\frac{1}{2} \text{Im} \left\{ \int_0^1 \right. \\ &\quad \left[ \left( \sin((\beta + \gamma)s + j\kappa) + \sin((\beta - \gamma)s + j\kappa) \right) \text{Si}(\beta(s + 1 + j\kappa)) \right. \\ &\quad + \left( \cos((\beta + \gamma)s + j\kappa) + \cos((\beta - \gamma)s + j\kappa) \right) \text{Ci}(\beta(s + 1 + j\kappa)) \\ &\quad + \left( \sin((\beta + \gamma)s - j\kappa) + \sin((\beta - \gamma)s - j\kappa) \right) \text{Si}(\beta(s - 1 - j\kappa)) \\ &\quad \left. \left. + \left( \cos((\beta + \gamma)s - j\kappa) + \cos((\beta - \gamma)s - j\kappa) \right) \text{Ci}(\beta(s - 1 - j\kappa)) \right] ds \right\} \\ &= -\frac{1}{2} \text{Im} \left\{ I_4(\beta + \gamma, \beta, j\kappa, 1 + j\kappa) + I_4(\beta + \gamma, \beta, -j\kappa, -1 - j\kappa) \right. \\ &\quad \left. + I_4(\beta - \gamma, \beta, j\kappa, 1 + j\kappa) + I_4(\beta - \gamma, \beta, -j\kappa, -1 - j\kappa) \right\}, \end{aligned} \quad (28)$$

and where

$$\begin{aligned} I_4(q, \beta, z_1, z_2) &= \int_0^1 [\sin(qs + \beta z_1) \text{Si}(\beta s + \beta z_2) + \cos(qs + \beta z_1) \text{Ci}(\beta s + \beta z_2)] ds \\ &= \frac{1}{q} \left[ \sin(\beta z_1 + q) \text{Ci}(\beta(1 + z_2)) - \cos(\beta z_1 + q) \text{Si}(\beta(1 + z_2)) \right. \\ &\quad - \sin(\beta z_1) \text{Ci}(\beta z_2) + \cos(\beta z_1) \text{Si}(\beta z_2) \\ &\quad + \cos(\beta z_1 - qz_2) \left( \text{Si}((\beta - q)(1 + z_2)) - \text{Si}((\beta - q)z_2) \right) \\ &\quad \left. - \sin(\beta z_1 - qz_2) \left( \text{Ci}((\beta - q)(1 + z_2)) - \text{Ci}((\beta - q)z_2) \right) \right]. \end{aligned} \quad (29)$$

To derive (29), we utilized the trigonometric addition formulas and the integration formulas 5.31 and 5.32 in [14]. Summarizing, we obtain

$$\begin{aligned} K_{mn} &= -\frac{1}{\pi} \text{Im} \left\{ I_4((n+m)\pi, n\pi, j\kappa, 1 + j\kappa) + I_4((n+m)\pi, n\pi, -j\kappa, -1 - j\kappa) \right. \\ &\quad \left. + I_4((n-m)\pi, n\pi, j\kappa, 1 + j\kappa) + I_4((n-m)\pi, n\pi, -j\kappa, -1 - j\kappa) \right\}. \end{aligned} \quad (30)$$

### 3.4 Cases $m = n > 0$

In cases when  $m = n > 0$  the last two terms in (30) are not suitable for numerical evaluation, since in the final expression in (29) the limit  $q \rightarrow 0$  must be taken. Alternatively, we can start with setting  $q = 0$  in the integrand in (29); the result reduces to

$$\begin{aligned} K_{nn} &= -\frac{1}{\pi} \operatorname{Im} \left\{ I_4(2n\pi, n\pi, j\kappa, 1 + j\kappa) + I_4(2n\pi, n\pi, -j\kappa, -1 - j\kappa) \right. \\ &\quad + \sin(jn\pi\kappa) \int_0^1 \left( \operatorname{Si}(n\pi(s + 1 + j\kappa)) - \operatorname{Si}(n\pi(s - 1 - j\kappa)) \right) ds \\ &\quad \left. + \cos(jn\pi\kappa) \int_0^1 \left( \operatorname{Ci}(n\pi(s + 1 + j\kappa)) - \operatorname{Ci}(n\pi(s - 1 - j\kappa)) \right) ds \right\} \\ &= -\frac{1}{\pi} \operatorname{Im} \left\{ I_4(2n\pi, n\pi, j\kappa, 1 + j\kappa) + I_4(2n\pi, n\pi, -j\kappa, -1 - j\kappa) \right. \\ &\quad + j \sinh(n\pi\kappa) \left( (2 + j\kappa) \operatorname{Si}(n\pi(2 + j\kappa)) - j\kappa \operatorname{Si}(jn\pi\kappa) \right) \\ &\quad \left. + \cosh(n\pi\kappa) \left( (2 + j\kappa) \operatorname{Ci}(n\pi(2 + j\kappa)) - j\kappa \operatorname{Ci}(jn\pi\kappa) - j\pi \right) \right\}. \end{aligned} \quad (31)$$

## 4 Numerical calculations

The here presented improved expansion is most useful at small separations, wherefore we restrict our study to values  $\kappa \leq 0.01$ ; results obtained at larger separations are readily available in the literature, with some of the most accurate in [2, 3].

The value of the truncation number  $N$  is mainly dictated by the computational resources at hand. Here, we have used a maximum value of  $N = 15000$ , at the smallest separations.

All our results will be presented in terms of the normalized capacitance  $\mathcal{C} = C / (4\epsilon_0 a)$ , where  $4\epsilon_0 a$  is the capacitance between two infinitely separated disks. Hence, it follows from (11) that  $\mathcal{C} = f_0$ .

### 4.1 Extrapolation schemes

To improve our numerical results, we have employed extrapolation.

#### 4.1.1 Power law model

First, we considered a simple power law model for the capacitance:

$$f_0(N) = \hat{\mathcal{C}} - \beta (N\kappa)^{-\alpha}, \quad (32)$$

where  $f_0(N)$  is the result obtained when using the truncation  $N$  in Equation (10),  $\hat{\mathcal{C}}$  is the extrapolated estimate in the limit  $N \rightarrow \infty$ ;  $\alpha$  and  $\beta$  (assuming  $\alpha > 0, \beta > 0$ ) are coefficients that are determined together with  $\hat{\mathcal{C}}$ .

$\kappa$	$N\kappa = 0.2$				$N\kappa = 1$			
	$f_0(N)$	$\hat{\mathcal{C}}$	$\alpha$	$\beta \cdot 10^2$	$f_0(N)$	$\hat{\mathcal{C}}$	$\alpha$	$\beta \cdot 10^3$
0.01	80.235	80.539	1.380	3.30	80.4312	80.4363	2.358	5.15
0.005	158.937	159.240	1.431	3.03	159.1384	159.1436	2.377	5.14
0.002	394.778	395.078	1.472	2.81	394.9827	394.9878	2.384	5.16
0.001	787.647	787.946	1.486	2.73	787.8533	787.8585	2.386	5.16
0.0005	1573.217	1573.516	1.492	2.71	1573.4238	1573.4290	2.388	5.16
0.0002	3929.640	3929.849	1.496	2.69	3929.8466	3929.8518	2.389	5.16
0.0001	7856.804	7857.102	1.498	2.69	7857.0105	7857.0156	2.391	5.15

**Table 1:** The extrapolation parameters,  $\alpha, \beta$  and  $\hat{\mathcal{C}}$ , obtained when fitting the power law extrapolation model (32) to  $f_0(N)$ ,  $f_0(N/2)$  and  $f_0(N/3)$ . The estimate of the true capacitance is  $C = 4\varepsilon_0 a \hat{\mathcal{C}}$

In our initial tests, the extrapolation parameters,  $\alpha, \beta, \hat{\mathcal{C}}$ , were determined by fitting (32) to  $f_0(N)$ ,  $f_0(N/2)$  and  $f_0(N/3)$  (using rounded values for the fractions of  $N$  when necessary). In Table 1 we present our results, for various separations  $\kappa$ , for two different values of the product  $N\kappa$ .

An important observation in Table 1 is that for constant values of  $N\kappa$  the values of the parameters  $\alpha$  and  $\beta$  are approximately constant, regardless of the value of  $\kappa$ . This is especially true for  $N\kappa = 1$ , but also for the smaller  $\kappa$ -values when  $N\kappa = 0.2$ . The results for  $N\kappa = 0.2$  (farther from convergence) and  $N\kappa = 1$  (closer to convergence) together indicate that the extrapolation scheme over-estimates the capacitance. Another observation from the data in Table 1 is that for each value of  $N\kappa$  the amount of extrapolation is approximately the same, regardless of the value of  $\kappa$ .

#### 4.1.2 Heuristic model for improvement at low accuracies

Considering decreasing separations  $\kappa$ , the limitation of the truncation  $N$  will eventually force us to use smaller values of  $N\kappa$ , which will push us farther from convergence. However, the properties of the convergence, as demonstrated in Table 1, offer an opportunity to improve poorly converged results, by using the following heuristic model:

$$f_0(N) = \hat{\mathcal{C}} + h(N\kappa), \quad (33)$$

where the term  $-\beta(N\kappa)^{-\alpha}$  in (32) has been replaced by a general function  $h(N\kappa)$ . Using Equation (33), we have developed a heuristic extrapolation method that is based on the assumption that when going from one  $\kappa$ -value to the next smaller value the function  $h$  remains almost unchanged. To verify this, we have compared the  $h$ -functions obtained at three different values of  $\kappa$ . We used equation (33), setting  $\tilde{\mathcal{C}} = \hat{\mathcal{C}}$ , with  $\hat{\mathcal{C}}$  taken from the seventh column in Table 1. The results are given in Figure 2, as function of  $(N\kappa)^{-1}$  for the values between the ones in Table 1. The  $h$ -functions in Figure 2 essentially illustrate the convergence, with higher degree of convergence at lower  $(N\kappa)^{-1}$  values, where the  $h$ -values at  $(N\kappa)^{-1} = 1$  indicate the amount left to extrapolate. The three curves are essentially occupying the same distance, especially those at the smaller separations  $\kappa = 0.001$  and  $\kappa = 0.0001$ , and for easier comparison we have included a magnification of the curves.

The nearly overlapping curves indicate that the convergence of the matrix inversion is determined mainly by the product  $N\kappa$ .

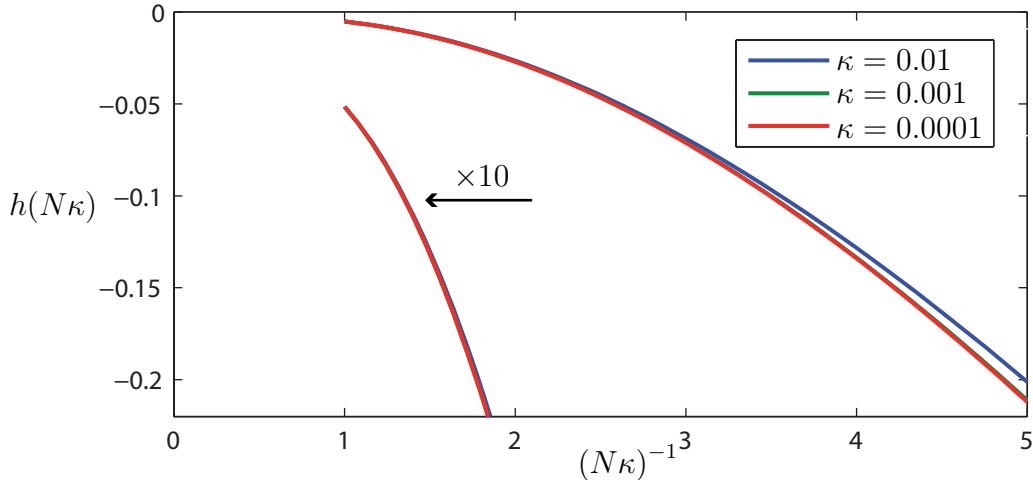


**Figure 2:** Comparison of the estimated  $h$ -functions, obtained from Equation (33), for three different orders of the separation  $\kappa$ . The  $h$ -function essentially indicates how close to convergence the calculation of  $C$  is, flatness of the curve for high  $N\kappa$  values indicates that  $C$  has essentially the distance  $|h(N\kappa)|$  left to its approximately true value.

Now, having confirmed the assumption, the heuristic extrapolation method works as follows:

1. Order the considered  $\kappa$ -values as  $\kappa_0 > \kappa_1 > \kappa_2 > \dots$ , with  $N, f_0(N), \tilde{C}$  and  $h$  indexed analogously.
2. Starting with  $\kappa_0$ , for which we already can assume a fairly good convergence by using a moderate number of expansion functions (see Figure 2), and using the power law (32), with a truncation number  $N_0$ , we obtain the extrapolation  $\hat{C}_0$ . This is taken as the starting value,  $\tilde{C}_0 = \hat{C}_0$ , for our improved algorithm, which from now proceeds repetitively:
3. Increment the index (denoted  $i$ ). Use equation (33) to find the  $h$ -function from the previous step:

$$h_{i-1}(N_{i-1}\kappa_{i-1}) = f_{0,i-1}(N_{i-1}) - \tilde{C}_{i-1}. \quad (34)$$

Let  $n_{i-1}$  be a truncation number fulfilling

$$N_i\kappa_i = n_{i-1}\kappa_{i-1}. \quad (35)$$

Assuming that  $h_i = h_{i-1}$ , it follows from (33) and (35) that

$$f_{0,i}(N_i) - \tilde{C}_i = f_{0,i-1}(n_{i-1}) - \tilde{C}_{i-1} = f_{0,i-1}\left(\frac{\kappa_i}{\kappa_{i-1}}N_i\right) - \tilde{C}_{i-1}, \quad (36)$$

from which the extrapolated capacitance becomes

$$\tilde{\mathcal{C}}_i = f_{0,i}(N_i) + \tilde{\mathcal{C}}_{i-1} - f_{0,i-1}\left(\frac{\kappa_i}{\kappa_{i-1}}N_i\right). \quad (37)$$

Note that  $n_{i-1}$ , determined from (35), must fulfil  $n_{i-1} \leq N_{i-1}$ , and if  $n_{i-1}$  does not become an integer the last term in (37) must be evaluated by interpolation between the adjacent integer values.

4. Repeat step 3 until the final (smallest)  $\kappa$ -value has been considered.

## 4.2 Results for the capacitance

At small separations, the first approximation to the capacitance is the geometric capacitance  $\mathcal{C}_g = \pi/(4\kappa)$ . A much better approximation is the result by Kirchhoff [10]:

$$\mathcal{C}_k \approx \frac{\pi}{4\kappa} + \frac{1}{4} \ln\left(\frac{1}{\kappa}\right) + \frac{1}{4} [\ln(16\pi) - 1] + o(1). \quad (38)$$

This formula, which has been proved rigourously by Hutson [11], becomes increasingly accurate as  $\kappa$  decreases.

Our results are divided into two cases. In the first case, we used a constant value  $N\kappa = 3$ , and considered separations down to  $\kappa = 0.0002$ ; the results are given in Table 2. Here, all extrapolations,  $\hat{\mathcal{C}}$ , were obtained by fitting the power law (32) to the  $f_0$ -values at  $N, N/2, N/3$ . We also present the relative excess  $(\hat{\mathcal{C}} - \mathcal{C}_g)/\mathcal{C}_g$  over the geometric capacitance. Our results are compared with the Kirchhoff result (38) and with the numerical results in [2, 3].

$\kappa$	$N$	$f_0(N)$	$\hat{\mathcal{C}}$	Exc. $\mathcal{C}_g$	Eq.(38)	Ref. [2]	Ref. [3]
0.01	300	80.43440	80.43451	2.41 %	80.42044	80.4342	80.43
0.005	600	159.14169	159.14179	1.31 %	159.13354	159.13	159.1
0.002	1500	394.98596	394.98607	5.82 %	394.98206	394.87	395
0.001	3000	787.85661	787.85672	3.13 %	787.85443	787.6	787
0.0005	6000	1573.42707	1573.42718	1.67 %	1573.42588	1573	
0.0002	15000	3929.84994	3929.85005	7.28 %	3929.84944	3928.9	

**Table 2:** Numerically calculated capacitances, where  $f_0(N)$  is the non-extrapolated value and  $\hat{\mathcal{C}}$  is the extrapolant. The estimated true capacitance is  $C = 4\epsilon_0 a \hat{\mathcal{C}}$ .

In the second case, we considered even smaller separations, down to  $\kappa = 0.00001$ ; the results are presented in Table 3. Since limited computer memory enforced a maximum truncation number  $N = 15000$ , all extrapolations were obtained with our heuristic method. As the starting value for the repetitive extrapolation, we took the  $\hat{\mathcal{C}}$ -value obtained at the smallest separation considered in Table 2, i.e.  $\kappa_0 = 0.0002, \hat{\mathcal{C}}_0 = 3929.85005$ ; see Section 4.1.2.

At the largest separation,  $\kappa = 0.01$ , our result agrees better with the reference numerical results than with (38), but for the smaller separations our results are more close to (38).

$\kappa$	$N$	$f_0(N)$	$\tilde{C}$	Exc. $\mathcal{C}_g$	Eq.(38)	Ref. [2]
0.0001	15000	7857.01294	7857.01378	3.86 %	7857.01355	7855.9
0.00005	15000	15711.16055	15711.16855	2.04 %	15711.16847	
0.00002	15000	39273.25402	39273.34241	0.87 %	39273.34244	
0.00001	15000	78543.05664	78543.42381	0.46 %	78543.42390	

**Table 3:** Numerically calculated capacitances, where  $f_0(N)$  is the non-extrapolated value and  $\tilde{C}$  is the extrapolant.

In Figure 3, we have plotted the difference between our results and the Kirchhoff result, which in effect is our numerical approximation of the rest term in Equation (38). For  $0.0002 \leq \kappa \leq 0.01$  the difference is positive and decreases with  $\kappa$  with the approximate behavior  $\propto \kappa^{0.8}$ , but when reaching the smallest  $\kappa$ -values the difference turns negative and increases in magnitude. This cannot by itself be taken as an error, since (38) is not the exact solution, neither a lower bound, but a solution that becomes increasingly accurate as  $\kappa$  decreases.

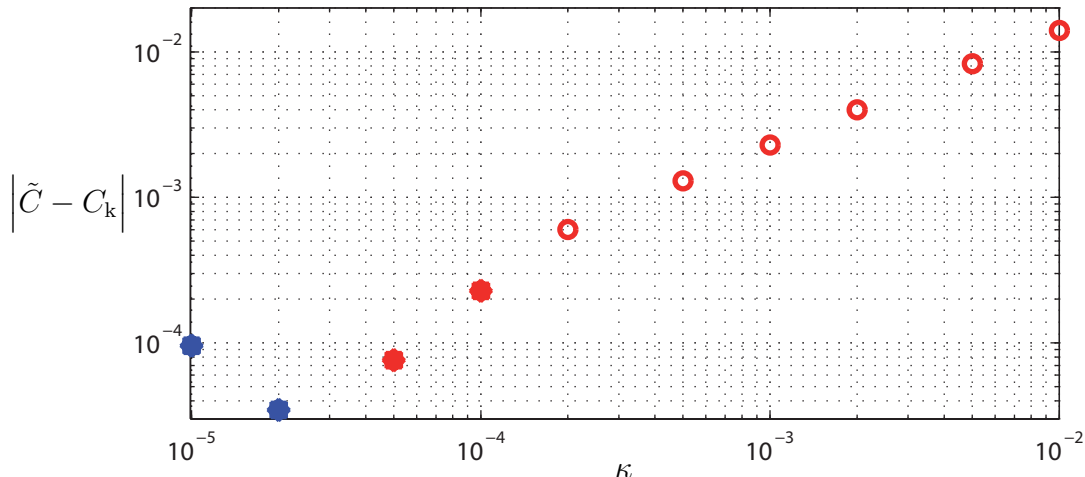


**Figure 3:** The magnitude of the difference between our extrapolated results and the Kirchhoff results from (38), as function of the relative separation  $\kappa$ . Red and blue colors denote positive and negative differences, respectively. The circles are the results from Table 2 and the dots are the results from Table 3.

We should also mention the result by Ignatowsky [2, 15], which differs from Kirchhoff's result in that the constant term is replaced by  $(\ln 8 - 1/2)/4$ , thereby falling below the Kirchhoff result by the amount of approximately 0.33447. Pólya and Szegő [16] have shown that Ignatowsky's result is a sharp lower bound for the capacitance. Thus, we see in Table 3 that at  $\kappa = 0.00001$  our non-extrapolated result is below this lower bound, which is an indication that convergence has not been reached due to an insufficient number of expansion functions. However, the extrapolated result is above the sharp lower bound.

### 4.3 On the accuracy of the results

Our numerical simulations have shown that for a fixed  $\kappa$  the unextrapolated capacitance  $f_0(N)$  increases with  $N$ , and from Tables 1 and 2 it appears that when using the power law extrapolation formula (32) the extrapolated value  $\hat{C}$  decreases with  $N$ . If we in Table 1 use the  $\hat{C}$ -values at  $N\kappa = 1$  as references, the extrapolations obtained at  $N\kappa = 0.2$  overestimate the references with about one third of the total amount of extrapolation. Similarly, if we in Table 2 use the  $\hat{C}$ -values at  $N\kappa = 3$  as references, the extrapolations obtained at  $N\kappa = 1$  (in Table 1) overestimate the references with about one third of the total amount of extrapolation. Applying this rule to the values in Table 2, we conclude that the true values are approximately  $4 \cdot 10^{-5}$  below the extrapolated value.

Using the subsequent repeated extrapolation, the error obtained at  $\kappa = 0.0002$  is propagated to the lower  $\kappa$ -values. If the extrapolation scheme was ideal, i.e. if the  $h$ -function in (33) was the same regardless of  $\kappa$ , no further contributions to the error would occur. To get a very rough estimate of the cumulated errors, we can study the similarities between the curves in Figure 2. Given the excellent agreement between the curves at the smaller  $\kappa$ -values, a pessimistic estimate is that the cumulated error is within 1/10 of the amount of extrapolation. Applying this estimate to the values given in Table 3 we obtain the estimate of the maximum error, denoted  $\Delta C$ , acquired in each step of the interpolation scheme. The results, rounded upward to one significant digit, are presented in Table 4. Since we typically have to let  $N\kappa$  decrease with  $\kappa$ , the most significant contribution to the accumulated error at a certain  $\kappa$ -value is acquired in the last step of the extrapolation scheme.

$\kappa$	0.0002	0.0001	0.00005	0.00002	0.00001
$\Delta C$	$4 \cdot 10^{-5}$	$8 \cdot 10^{-5}$	$8 \cdot 10^{-4}$	$9 \cdot 10^{-3}$	$4 \cdot 10^{-2}$

**Table 4:** Estimated order of the cumulated error during each step of the heuristic extrapolation scheme.

## 5 Conclusions

By expanding the kernel in the Love equation into a Fourier cosine series, with the coefficients expressed analytically in terms of Sine and Cosine integrals, we have increased the accuracy of the expansion, making it possible to use considerably larger truncation numbers  $N$  than in previous studies. In this way, we have improved the numerical values for the capacitance at small plate separations  $\kappa$ .

The present method enable us to consider smaller plate separation distances than has been considered before, while maintaining a high accuracy. Numerical tests indicated that the degree of convergence is determined by the product  $N\kappa$ . Hence, for this method of calculating the capacitance it becomes practically impossible to accommodate for a decreasing plate separation by a corresponding increase of the number of expansion functions; cf. Figure 2. To compensate for this problem, we have developed a heuristic extrapolation scheme that uses the information obtained at intermediate separations, where the convergence is good, to improve the convergence at small separations.

At larger separations,  $\kappa$ , than those considered in our study, convergence is obtained for smaller numbers,  $N$ , of expansion functions. In such cases, one does not need to use the analytical results in Section 3 for the integrals, since they can instead be calculated accurately by means of numerical methods [2, 3]. In fact, for large  $\kappa$ -values the explicit expressions in Section 3 are unsuitable for numerical evaluation. This can be seen by observing that from (9) and (4) it follows that for any  $\kappa > 0$  the matrix elements fulfil the relation

$$|K_{mn}| \leq 2K_{0,0} < 2 \quad (39)$$

and that when we tested the algorithm for separations  $1 \leq \kappa \leq 10$  we encountered spurious large matrix elements violating the condition (39). The reason is that when  $N\kappa \gg 1$ , the individual terms in the expressions given in Section 3 exhibit an exponential growth  $\propto e^{N\kappa}$  and the condition (39) is met by taking the differences between such very large terms, but numerically this kind of evaluation leads to cancelation effects.

## References

- [1] E. R. Love, “The Electrostatic Field of Two Equal Circular Co-Axial Conducting Disks” *Quart. J. Mech. and Appl. Math.*, **2**, 428-451, 1949.
- [2] H. J. Wintle and S. Kurylowicz, “Edge Corrections for Strip and Disc Capacitors” *IEEE Trans. Instr. and Meas.*, **34**(1), 41-47, March 1985.
- [3] G. T. Carlson and B. L. Illman, “The circular disk parallel plate capacitor” *Am. J. Phys.*, **62**(12), 1099-1105, December 1994.
- [4] H. Nishiyama and M. Nakamura, “Capacitance of Disk Capacitors” *IEEE Trans. Comp., Hybrids., and Manuf.*, **16**(3), 360-366, 1993.
- [5] C. Donolato, “Approximate evaluation of capacitances by means of Green’s reciprocal theorem” *Am. J. Phys.*, **64**(8), 1049-1054, August 1996.
- [6] C.-O. Hwang and J. A. Given, “Last-passage Monte Carlo algorithm for mutual capacitance” *Phys. Rev. E*, **74**, 027701, 2006.
- [7] S. E. El-Genid, “Chebyshev solution of differential equations” *Comput. J.*, **12**, 282-287, 1969.
- [8] <[http://en.wikipedia.org/wiki/Clenshaw–Curtis\\_quadrature](http://en.wikipedia.org/wiki/Clenshaw–Curtis_quadrature)>
- [9] G. T. Carlson and B. L. Illman, “Series capacitors and the inverse sum rule” *Am. J. Phys.*, **70**(11), 1122-1128, November 2002.
- [10] G. Kirchhoff, “Zur theorie des kondensators” *Monatsb. Acad. Wiss. Berlin*, 731-734, 1877.
- [11] V. Hutson, “The circular plate condenser at small separations” *Proc. Camb. Phil. Soc.*, **59**, 211-224, 1963.

- [12] I. N. Sneddon, *Mixed Boundary Value Problems in Potential Theory*, Wiley, New York, 1966.
- [13] M. Abramowitz and I. A. Stegun, *Handbook of Mathematical Functions with Formulas, Graphs, and Mathematical Tables*, Dover, New York, 1964.
- [14] I. S. Gradshteyn and I. M. Ryzhik, *Table of Integrals, Series and Products*, Academic Press, New York, 1980.
- [15] W. Ignatowsky, “Kreisscheibenkondensator”, *Acad. Sci. URSS Trav. Inst. Steklov*, series 2, **3**, 1-104, 1932.
- [16] G. Pólya and G. Szeg, *Isoperimetric inequalities in mathematical physics*, Princeton, 1951.